Journal of Applied Mechanics and Technical Physics, Vol. 36, No. 3, 1995

IGNITION OF PULVERIZED COAL PARTICLES IN SHOCK WAVES

S. P. Kiselev and V. P. Kiselev

UDC 662.612.32

The paper reports the results of numerical simulation of the behavior of pulverized coal particles in shock waves. Heating of gas in a cloud of particles has been shown to result in ignition of the particles in the passing shock waves. A vortex flow has been observed to form behind a shock wave reflected from the back wall of a channel.

Let us consider a tenuous cloud of solid spherical particles, occupying a region Ω_2 (Fig. 1), onto which a shock wave comes from the left. The gas flow is described by the Euler equations in Ω_1 and by equations of a continuum-discrete model in Ω_2 [1, 2]. Choosing the x axis in the direction of shock-wave propagation and the y axis perpendicular to that direction, we write the system of equations of gas and particles in the plane case [1, 2]:

$$\frac{\partial f}{\partial t} + v_2\frac{\partial f}{\partial x} + w_2\frac{\partial f}{\partial y} + \frac{\partial}{\partial v_2}(a_x f) + \frac{\partial}{\partial w_2}(a_y f) + \frac{\partial}{\partial T_2}(qf) = 0,$$

$$f = f(t, x, y, v_2, w_2, r, T_2), \quad n = \int f\,dV, \quad m_2 = \frac{4}{3}\pi\int r^3 f\,dV,$$

$$dV = dv_2\,dw_2\,dr\,dT_2, \quad m_1 + m_2 = 1, \quad q = 2\pi\lambda r \mathrm{Nu}\frac{T_1 - T_2}{c_s m_p},$$

$$a_x = \frac{v_1 - v_2}{\tau} - \frac{1}{\rho_{22}}\frac{\partial p}{\partial x}, \quad a_y = \frac{w_1 - w_2}{\tau} - \frac{1}{\rho_{22}}\frac{\partial p}{\partial y}, \tag{1}$$

$$\frac{1}{\tau} = \frac{3}{4}\left(\frac{\mathrm{Re}\,\mu}{\rho_{22}d^2}\right)C_d(\mathrm{Re}, \mathrm{M}_{12}), \quad m_p = \frac{4}{3}\pi r^3\rho_{22},$$

$$C_d(\mathrm{Re}, \mathrm{M}_{12}) = \left(1 + \exp -\frac{0{,}43}{\mathrm{M}_{12}^{4{,}67}}\right)\left(0{,}38 + \frac{24}{\mathrm{Re}} + \frac{4}{\sqrt{\mathrm{Re}}}\right), \quad \mathrm{Re} = \frac{\rho_{11}|\mathbf{v}_1 - \mathbf{v}_2|d}{\mu},$$

$$\mathrm{M}_{12} = \frac{|\mathbf{v}_1 - \mathbf{v}_2|}{c}, \quad c = \sqrt{\frac{\gamma p}{\rho_{11}}}, \quad \mathrm{Nu} = 2 + 0{,}6\,\mathrm{Re}^{0{,}5}\mathrm{Pr}^{0{,}33}, \quad \mathrm{Pr} = \frac{c_p\mu}{\lambda}, \quad \mathcal{E}_1 = c_V T_1,$$

$$\frac{\partial\varphi}{\partial t} + \frac{\partial F}{\partial x} + \frac{\partial G}{\partial y} + \Phi = 0, \quad \rho_1 = \rho_{11}m_1, \quad p = (\gamma - 1)\rho_{11}\mathcal{E}_1,$$

$$\varphi = \begin{pmatrix} \rho_1 \\ \rho_1 v_1 \\ \rho_1 w_1 \\ \rho_1(\mathcal{E}_1 + (v_1^2 + w_1^2)/2) \end{pmatrix}, \quad F = \begin{pmatrix} \rho_1 v_1 \\ \rho_1 v_1^2 + p m_1 \\ \rho_1 v_1 w_1 \\ \rho_1 v_1 A_1 \end{pmatrix},$$

Institute of Theoretical and Applied Mechanics, Siberian Branch of the Russian Academy of Sciences, 630090, Novosibirsk. Translated from Prikladnaya Mekhanika i Tekhnicheskaya Fizika, No. 3, pp. 31-37, May-June, 1995. Original article submitted March 28, 1994; revision submitted April 8, 1994.

0021-8944/95/3603-0347$12.50

$$G = \begin{pmatrix} \rho_1 w_1 \\ \rho_1 v_1 w_1 \\ \rho_1 w_1^2 + p m_1 \\ \rho_1 w_1 A_1 \end{pmatrix}, \quad \Phi = \begin{pmatrix} 0 \\ \Phi_1 \\ \Phi_2 \\ A_2 \end{pmatrix},$$

$$A_1 = \mathcal{E}_1 + \frac{p m_1}{\rho_1} + \frac{(v_1^2 + w_1^2)}{2}, \quad \rho_{22} = \text{const},$$

$$A_2 = v_1 \Phi_1 + w_1 \Phi_2 + p\left(\frac{\partial m_1}{\partial t} + v_1 \frac{\partial m_1}{\partial x} + w_1 \frac{\partial m_1}{\partial y}\right) - \rho_1 \Phi_3,$$

$$\Phi_3 = \frac{1}{\rho_1} \int m_p \left(\frac{(v_1 - v_2)^2}{\tau} + \frac{(w_1 - w_2)^2}{\tau} - c_s q \right) f \, dV,$$

$$\Phi_1 = -p \frac{\partial m_1}{\partial x} + \int m_p \frac{v_1 - v_2}{\tau} f \, dV, \quad \Phi_2 = -p \frac{\partial m_1}{\partial y} + \int m_p \frac{w_1 - w_2}{\tau} f \, dV.$$

Here the index 1 denotes the parameters of the gas and index 2, those of the particles; f is the distribution function; v_1, w_1, ρ_{11}, ρ_1, T_1, p, γ, ε_1, and m_1 are the velocities along the x and y axes, the true density, the mean density, the temperature, the pressure, the adiabatic exponent, the specific internal energy, and the volume concentration of the gas; n is the calculated particle concentration; v_2, w_2, a_x, a_y, ρ_{22}, r, T_2, and m_2 are the velocity and acceleration along the x and y axes, the true density, the radius, the temperature, and the volume concentration of particles; μ, λ c_V, and c are the viscosity, the thermal conductivity, the heat capacity, and the velocity of sound in the gas; c_s is the heat capacity of the material of the particles; Re, Nu, Pr, and M_{12} are the Reynolds, Nusselt, Prandtl, and Mach numbers.

The system of equations (1) was solved numerically on a personal computer. The gas equations were calculated on an Euler grid with the third order of accuracy and the kinetic equations were solved in Lagrange variables. In contrast to [2], the equations of the particle trajectories and heat transfer were integrated analytically in each time interval. This increased the accuracy of the calculation of the particles and removed the limitation on the time interval $\tau \leq \rho_{11} d^2/\mu$. For the gas, the hard-wall condition was imposed on γ_1, γ_3 and the symmetry condition, on γ_2, γ_4. For the particles, the condition of specular reflection was imposed on γ_1, γ_3 and the condition of particle absorption, on γ_2, γ_4 (see Fig. 1).

Let us consider the problem of ignition of coal particles in passing shock waves. The ignition of coal dust in passing shock waves and those reflected from the tube end was studied experimentally in [3, 4]. By approximating the experimental data we obtained an empirical formula for the ignition time τ_{ig} in shock waves reflected from the tube end; this formula differs from the corresponding formula in [3, 4] by the coefficients in front of the exponents and has the form

$$\tau_{ig} = 5{,}5 \cdot 10^{-7} \ln\left(\frac{V_g}{V_g - 0{,}04}\right) \exp\left(10^4/T_1\right) + \\ + 2 \cdot 10^{-9} V_g^{0,3} (1{,}25 p/p_0)^{-(1+3{,}7 V_g)} \exp\left(2{,}3 \cdot 10^4/T_1\right), \tag{2}$$

where $V_g = 0.55$ and $p_0 = 1$ atm. Using the temperature and pressure behind the passing shock wave, we showed that the τ_{ig} calculated from (2) is three orders of magnitude greater than the experimental value. It is of interest, therefore, to consider the problem of ignition of particles within the framework of the given model (1), supplemented with Eq. (2). We must note, however, that Eq. (2) was obtained in reflected shock waves for constant gas parameters p, T_1. Let us find the conditions for ignition of coal particles for the variables p, T_1. The probability of the particles igniting in a time dt is $dt/\tau_{ig}(p, T_1)$ and so the condition for particle ignition has the form

$$\int_0^{t^*} \frac{dt}{\tau_{ig}(p, T_1)} = 1.$$

Here the integral is taken along the particle trajectory, τ_{ig} is determined from Eq. (2), and t^* is the particle ignition time.

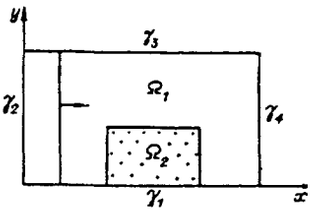

Fig. 1

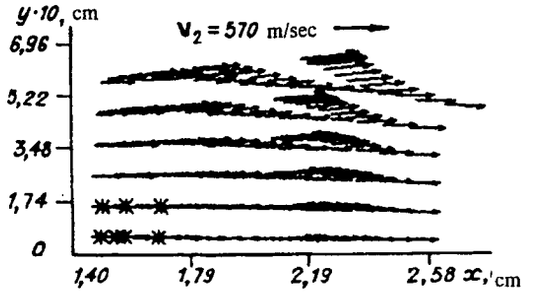

Fig. 2

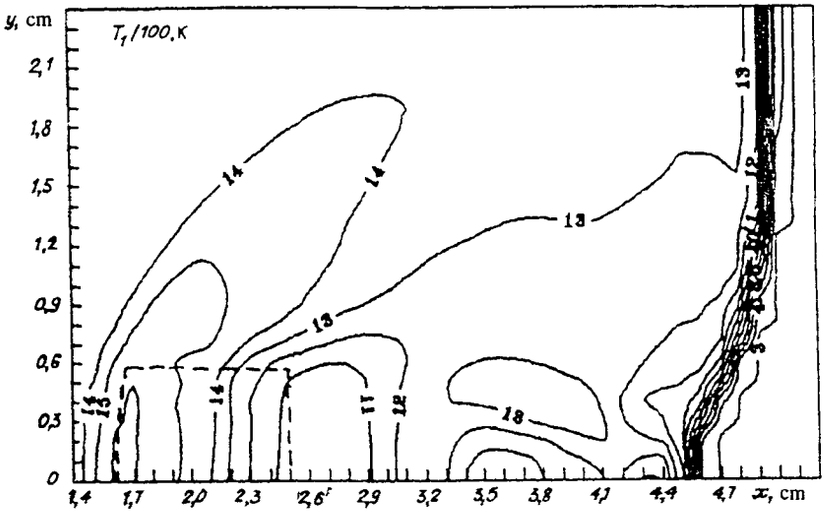

Fig. 3

At the time $t = 0$ the particles were in the region Ω_2, onto which a shock wave comes from the left (see Fig. 1). The size of the cloud is $\Delta y = 0.6$ cm in the y direction and $\Delta x = 1$ cm in the x direction. The cloud consisted of four fractions of coal particles with diameters $d_i = 10$, 20, 30, and 40 μm and the particle density was $\rho_{22} = 1.2$ g/cm^3. The volume concentration of each fraction was $m_2^{(i)} = 7 \cdot 10^{-4}$ and the total volume fraction was $m_2^0 = 2.8 \cdot 10^{-3}$. The choice of m_2^0 was dictated by the conditions of the experiment [3, 4], where the particles were introduced initially as a layer sprinkled densely on a substrate. When the shock wave passes the particles are blown off the substrate and form a tenuous cloud, in which the particles ignite. The tenuous cloud is optically transparent and so the volume concentration of the particles in it is less than $m_2^* \approx 3 \cdot 10^{-3}$ [4].

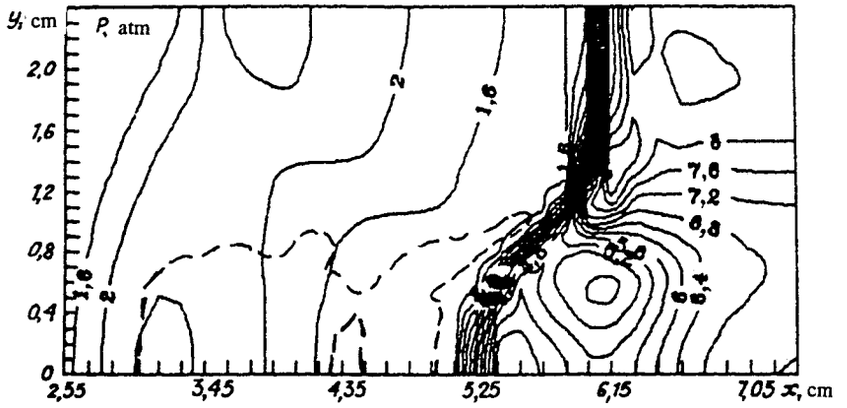

Fig. 4

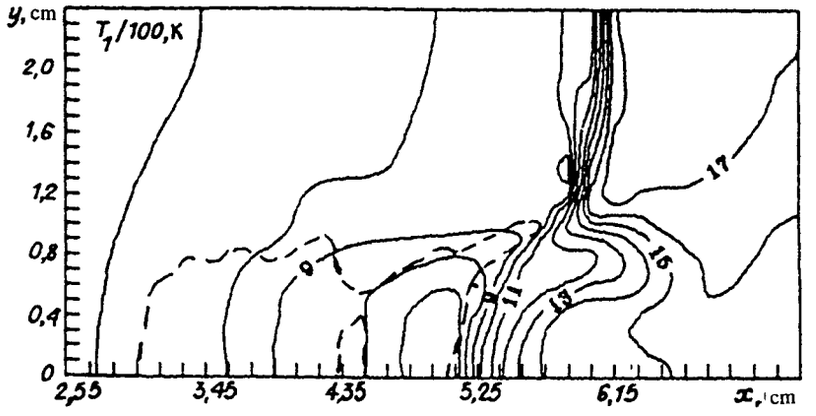

Fig. 5

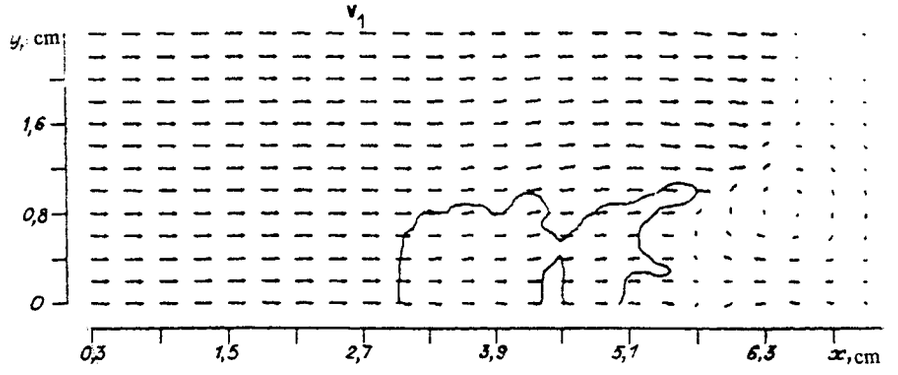

Fig. 6

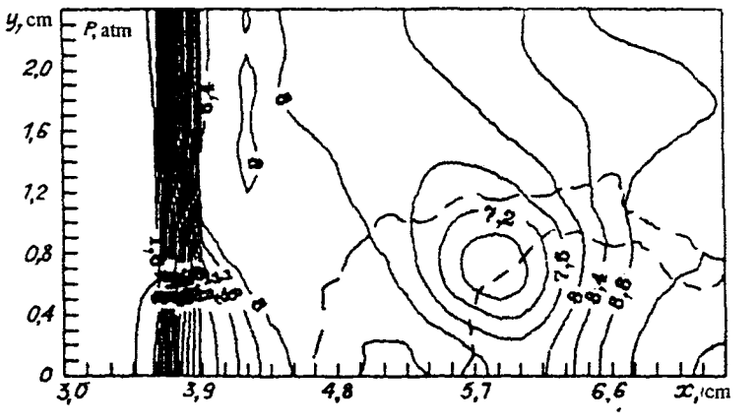

Fig. 7

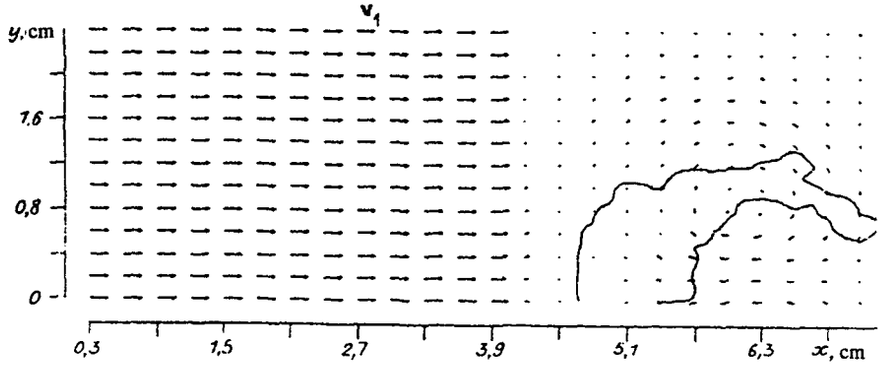

Fig. 8

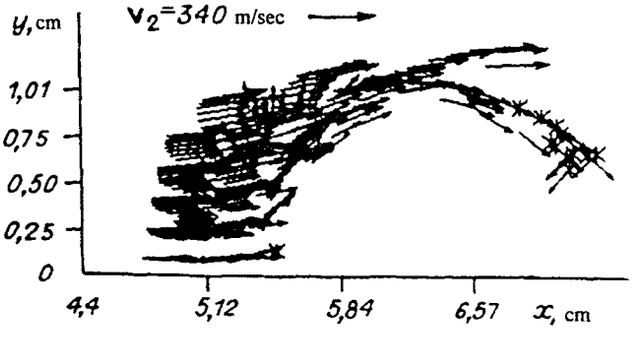

Fig. 9

This study does not consider processes that form the tenuous cloud and assumes that the cloud forms at the time t = 0. The gas parameters ahead of the shock waves are in keeping with [3, 4]: $\rho_{11}^0 = 1.4 \cdot 10^{-4}$ g/cm^3, $T_1^0 = 293$ K, $p^0 = 0.1$ atm, and the Mach number of the shock wave $M_0 = 4.6$. The calculations were done in the laboratory coordinate system.

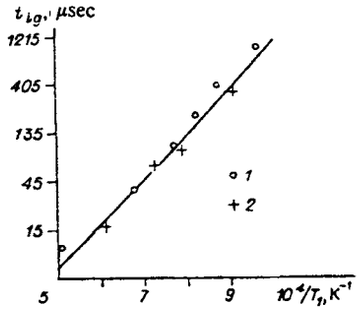

Fig. 10

The field of particle velocities at $t = 30$ μsec is shown in Fig. 2. The asterisks denote particles in which ignition occurred at $t \approx 30$ μsec. Figure 3 shows the gas isotherms $T_1(x, y)$ for $t = 30$ μsec, with the dashed line representing the boundary of the cloud. The particles are ignited in the region where the gas temperature rises to $T_1 = 1600$ K. The gas temperature behind the passing shock wave is $T_1 = 1300$ K. The temperature T_1 increases near the left boundary of the cloud because a compression wave forms ahead of the cloud and the Mach number $M_1 = v_1/c$ there decreases from 1.7 to 1.1. The flow accelerates to $M_1 = 1.3$ in the rarefaction wave formed inside the region and the temperature decreases to 1100 K. The temperature distribution inside the cloud, therefore, is substantially nonuniform.

A localized region of elevated temperature ($T_1 \approx 1400$ K) forms behind the cloud ($x \approx 3.5$ cm) because the flow is decelerated and turned by the wall $y = 0$. Along with the above formulation of the problem, we performed calculations when the initial conditions for the gas were given in the form of a homogeneous flow with the parameters of the gas behind the shock wave front. The results of the calculations were consistent with those given in Figs. 2 and 3. To evaluate the influence of m_2^0 on t^* we carried out calculations for $m_2^0 = 10^{-3}$ and the same shock wave parameters. As a result, the ignition delay time t^* increased to 90 μsec. The ignition of particles in passing shock waves thus is due to the deceleration of the gas flow by particles and a corresponding increase in the temperature in the particle cloud.

Let us consider the flow and ignition of coal particles behind a shock wave reflected from the end of the tube. The gas parameters ahead of a passing shock wave are the same as above and $M_0 = 3.6$. The condition $v_1 = 0$ and the conditions for the reflection of particles were the boundary conditions imposed on γ_4. Figures 4 and 5 show the isobars and isotherms at t = 100 μsec; a dashed line denotes the boundary of the cloud.

Figure 6 shows the velocity field of the gas for the same time, and the solid line corresponds to the boundary of the particle cloud. A vortex is seen to form behind a shock wave reflected from the wall. The vortex structure forms because the parameters of the gas behind the particle cloud are not uniform. Deceleration by particles makes the velocity of the gas near $y = 0$ lower than in the neighborhood of the top wall γ_3. As a result, the shock wave reflected from the wall propagates more rapidly for $y = 0$ than for $y \approx 2$ cm and an oblique wave arises, joining two direct waves. Since the pressure behind a direct shock wave is higher than behind an oblique wave, gas from the upper region of increased pressure begins to move to the lower region, being accelerated in the rarefaction wave. The gas then is decelerated by the lower wall and is turned into a vortex, which in turn increases the slope of the oblique shock wave.

Similar vortex flow occurs in the problem of viscous flow of gas behind a plate, flying from the surface of a body immersed in a supersonic stream [5]. The nonuniform flow field of gas ahead of the shock wave in this case is produced by the plate. After the reflected shock wave has passed through the cloud, its front straightens out (the oncoming stream ahead of the cloud becomes uniform). The vortex remains ahead of the cloud, being slowly attenuated because of viscous interaction with particles. This is clearly seen from Figs. 7 and 8, which show the isobars and velocity field of the gas for $t = 160$ μsec. By inertia the particles move to the right and, entering the region of reverse motion of gas in the vortex, they slow down and move upward (Fig. 9, which shows the velocity field of the particles for $t = 160$ μsec). The asterisks denote particles which ignited.

Figure 10 shows the dependence of the ignition time of coal particles on the gas temperature T_1 [points 1 correspond to the experiment of [3, 4], points 2 correspond to numerical computation, and the line is described by Eq. (2)]. The results of the calculations are in fairly good agreement with the experimental data.

In conclusion, we note that the formation of a vortex may play the determining role in lifting the coal dust behind reflected shock waves.

REFERENCES

1. S. P. Kiselev, G. A. Ruev, A. P. Trunev, et al., Shock-Wave Processes in Two-Component and Two-Phase Media [in Russian], Nauka, Novosibirsk (1992).
2. V. P. Kiselev, S. P. Kiselev, and F. M. Fomin, "On the interaction of a shock wave with a cloud of finite-dimensional particles," Prikl. Mekh. Tekh. Fiz., **35**, No. 2 (1994).
3. V. M. Boiko, A. N. Papyrin, and S. V. Poplavskii, "On the mechanism of the ignition of dust particles in passing shock waves," Fiz. Gor. Vzry., **29**, No. 3, 143 (1993).
4. S. V. Poplavskii, "Study of the nonstationary interaction of shock waves with dust-gas mixtures," Author's Abstract of Candidate's Dissertation, Novosibirsk (1992).
5. N. P. Gridnev," Structure of flow under viscous interaction of a shock wave with a flying particle," Prikl. Mekh. Tekh. Fiz., No. 2, 115 (1987).